Progress In Electromagnetics Research M, Vol. 112, 151–161, 2022

Iron Loss Calculation in Switched Reluctance Motor Based on Flux Integral Path Method

Kuo Li[1, *], Aide Xu[1], Bing Leng[2], Yang Yang[2], and Jinghao Sun[2]

Abstract—In this paper, a new fast and accurate method, the Flux Integral Path (FIP) method, is proposed for switched reluctance motor (SRM) to analyze the iron loss. The magnetic flux generated by stator poles is integrated over a period of time, then, the eddy current loss and the hysteresis loss of the whole SRM can be directly calculated by analyzing the path distribution of the flux closed loop without dividing the motor into four blocks (stator pole, stator yoke, rotor pole, and rotor yoke). The concept of flux flow is introduced to calculate the eddy current loss, and the piecewise linear fitting of flux density curve in the period is used to approximate the differential and simplify the hysteresis loss calculation. The FIP method can be well applied to non-sinusoidal and nonlinear magnetic density of SRM because of the combination of Finite Element Analysis (FEA) simulation. Furthermore, the loss separation model and Fast Fourier Transform (FFT) method were compared with the FIP method of the iron loss calculation, and the 2D FEA simulation results were used to verify the method proposed in this paper.

1. INTRODUCTION

Due to its unique double salient pole structure, strong fault tolerance, large starting torque, simple and firm structure, and other advantages, switched reluctance motor (SRM) has been more and more widely used in electric vehicles, mining industry, aerospace, and other fields [1–4]. However, the loss will be generated in the SRM when the motor is running, which has a significant impact on the performance index and efficiency of the SRM, and at the same time, the various losses will be lost in the form of heat. Especially the SRM is running under the condition of high speed or long time working, and the generation of heat is considerable, which will shorten the service life of the motor, even cause an accident in some cases. Therefore, it is very important to calculate the loss of SRM quickly and accurately.

The loss in SRM includes the following parts: winding copper loss, iron loss, mechanical loss, and stray loss. Because the current in phase windings changes constantly during the excitation, the induced magnetic field in the stator pole also changes periodically, and the changing magnetic field will produce iron loss in the whole motor. The accurate estimation of iron loss is particularly important to SRM, especially in the predesign stage, which directly affects the output power and stability of SRM. In addition, iron loss can be divided into eddy current loss and hysteresis loss. Eddy current loss is the energy loss caused by the eddy current flowing on the silicon steel sheet, and the hysteresis loss is caused by the vibration and friction between magnetic domains in the changing magnetic field.

At present, several methods to predict and calculate the iron loss for SRM have been proposed. In [5], Epstein frame was used to directly measure the iron loss, which is relatively simple. But due to the uneven magnetic field distribution, this method has low accuracy and large error. In [6], the influence of minor hysteresis loops was considered when the hysteresis loss is calculated, and a correction

Received 13 June 2022, Accepted 21 July 2022, Scheduled 4 August 2022

* Corresponding author: Aide Xu (aidexu@dlmu.edu.cn).

[1] School of Information Science and Technology, Dalian Maritime University, Dalian 116026, People's Republic of China. [2] School of Marine Electrical Engineering, Dalian Maritime University, Dalian 116026, People's Republic of China.

coefficient was introduced to quantify the effect. The paper [7] gave the analytical calculation method of flux density in each major part of SRM in the form of matrix. This method saves the time of magnetic field simulation, but introduces a large calculation error and does not consider the influence of flux saturation. Obviously, the internal flux of the motor is induced by the stator poles, due to the windings on them. So, the flux of stator pole was obtained by analytical formulas [8] and finite element analysis (FEA) method [9], respectively, and flux of the rest parts was derived, then the iron loss was calculated based on the flux density distribution. From the comparison of the two methods, it can be seen that the flux density obtained by the FEA method is closer to the actual running condition of the motor. In [10], the magnetic flux in the motor can be obtained analytically by Fourier transform from the phase currents and the air gap permeability model.

In [11], an iron loss model based on Steinmetz equation was proposed, the practical flux density waveform was compared with the sinusoidal waveform, and the equivalent coefficient was used to correct the calculated results. This method can calculate the core loss for non-sinusoidal magnetic density, although it is not precise enough. In [12], the eddy current and hysteresis losses were discretized into a limited number of elements according to the magnetic flux density distribution, and then the iron loss of the whole motor was obtained by means of the sum. In [13], the eddy current loss coefficient and hysteresis loss coefficient in the calculation formulas were defined by the flux density, respectively, and the above coefficients were expressed by fitting into the high-order form of power function.

In this paper, a more accurate and simpler calculation method of iron loss is proposed. Because the winding at the stator pole run through three-phase AC current, the flux is also periodic. Meanwhile, the stator pole is regarded as the "magnetic source" of the field in SRM, and the flux density within the period of time is integrated. Then the total flux path of switched reluctance motor is quantitatively analyzed, and the iron loss of SRM is investigated. In summary, the method proposed in this paper has the following characteristics:

1) In the calculation of iron loss, the influence of magnetic flux density change in core loss is considered in the form of integration, rather than only through peak flux density like most current methods.

2) From the perspective of flux path, the iron loss of SRM is calculated as a whole, instead of dividing the motor into stator pole, stator yoke, rotor pole, and rotor yoke to analyze flux density and core loss distribution, respectively.

3) Combined with the finite element analysis, the precise distribution and variation of flux density in the motor can be obtained, which makes the calculation of core loss more accurate and reliable.

2. THE FIP METHOD

Each phase winding of SRM turns on successively, which will inevitably lead to instability of the current in the process of commutation in the motor windings. Therefore, the distribution of magnetic field in the motor is also uneven and varies with time. As can be seen from Figure 1, the three-phase current has a nonsinusoidal waveform, especially in the commutation overlap region. Accordingly, the flux density of the excited phase in SRM is much higher than that of the non-excited phase (Figure 2), and at two different moments, with the change of the rotor position, the distribution of the flux density in SRM also changes a lot.

At present, a method widely used in the calculation of iron loss is the loss separation model in Steinmetz-form, as follows [14]:

$$P_{\text{iron}} = P_e + P_h = K_e f^2 B_P^2 + K_h f B_P^{\alpha} \tag{1}$$

where P_e and P_h are eddy current loss and hysteresis loss, respectively. K_e and K_h are eddy current loss and hysteresis loss coefficients, respectively. B_P is the peak value of the flux density, and f is the frequency of magnetization. α is called Steinmetz coefficient, which ranges from 1 to 2.

A large number of experiments and examples prove that the loss separation model can calculate the iron loss accurately when the flux density waveform is sinusoidal, but in the actual operation of SRM, the flux density in the core is usually non-sinusoidal. So, the model cannot be used directly in this case. On the other hand, SRM generally needs to be divided into four parts (stator pole, stator yoke, rotor pole, and rotor yoke) to calculate eddy current and hysteresis losses respectively in the loss

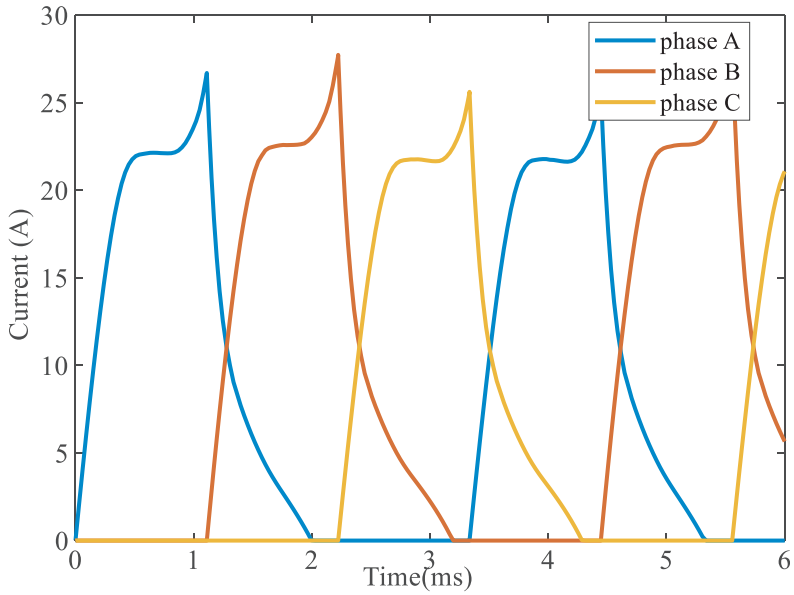

Figure 1. The three-phase currents in the motor turn on successively.

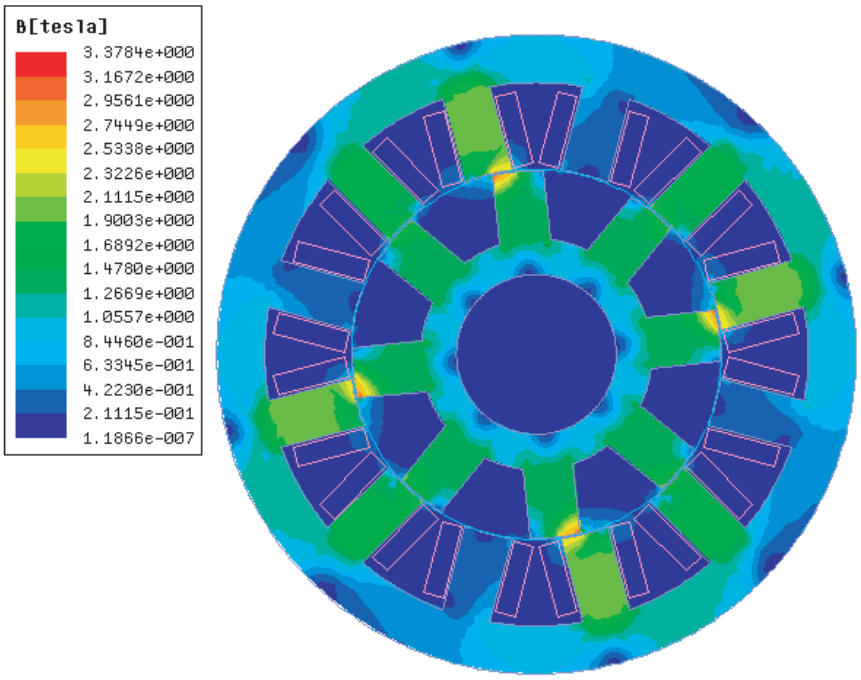

Figure 2. The distribution of magnetic flux density in SRM.

separation model, which will undoubtedly increase the work of calculation and also increase the error in this process.

For a three-phase 12/8 SRM, each phase winding is electrically conductive in turn. The flux induced in the stator pole of the excitation phase will form a closed loop mostly through the adjacent stator pole and rotor part, and a small fraction goes farther, as shown in Figure 3(a). Due to the absolute symmetry of SRM, the total flux path in a period is three times the flux path of a phase, i.e., 12 times the flux path of a stator pole excitation.

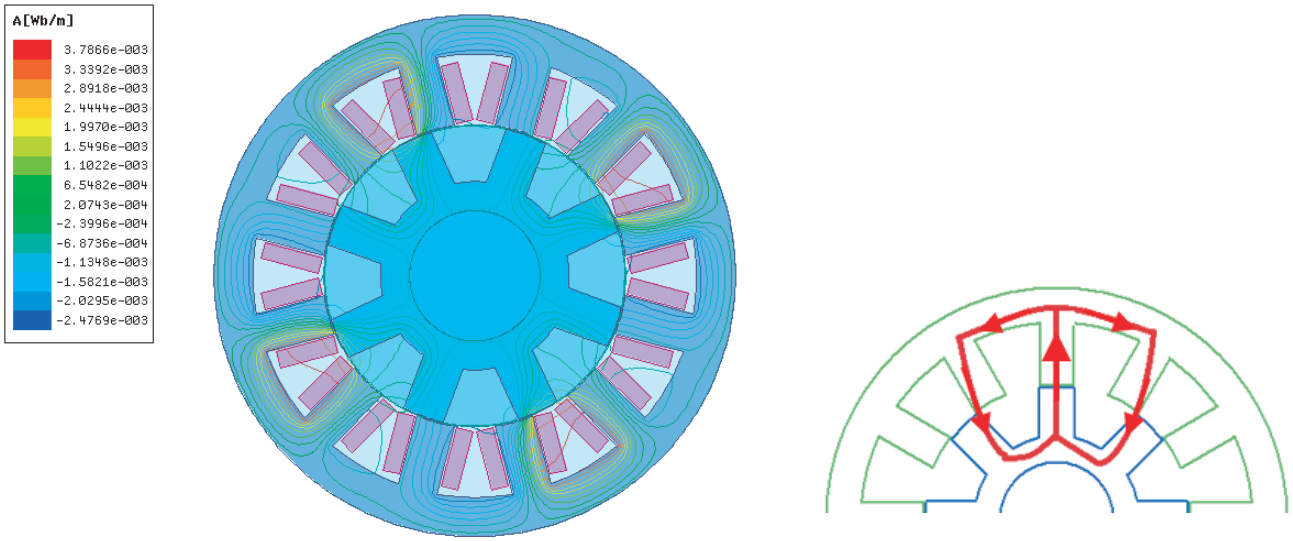

(a) (b)

Figure 3. Quantization of flux path. (a) Magnetic field line distribution. (b) The abstract flux path of the excited stator pole in SRM.

Next, the flux path in SRM will be quantified. Magnetic flux generated by the excitation phase will return to the excitation pole through the stator yoke, adjacent stator poles, rotor poles, and rotor yoke, which is the flux path. In general, the two sides of the excitation stator poles are the possible path of the flux, as shown in Figure 3(b). At different rotor positions, the distribution of the flux on both sides is different, and there is a large fluctuation. If the adjacent stator pole of the excitation phase is located near the center line of the rotor slot, there is almost no magnetic flux distribution on the stator pole, and the flux mainly forms a closed loop through the other side of the stator pole. However, if we consider the overall magnetic flux, the flux paths on both sides of the excitation phase can be equivalent to one path: a stator pole and a rotor pole.

The effect of air gap on flux is ignored in order to simplify the analysis. Therefore, the flux path length of a single excited stator pole can be calculated by

$$L = \frac{\pi}{N_S} + \beta d_s + \frac{\pi}{N_R} + \gamma D_r + D_s - d_r \tag{2}$$

where D_S and d_S are the outer diameter (m) and inner diameter (m) of the stator, respectively. D_r and d_r are the outer diameter (m) and inner diameter (m) of the rotor, respectively. β is the stator pole arc coefficient; γ is the rotor pole arc coefficient; N_S and N_R are the number of the stator poles and rotor poles, respectively.

Therefore, through the above quantization method of magnetic flux path, the calculation of iron loss can avoid discussing the flux density distribution in different parts of the SRM, and there is no need to calculate the iron loss of each part of SRM separately.

Based on the above analysis and quantification of flux path, the calculation methods of eddy current and hysteresis losses are given below, respectively.

2.1. Eddy Current Loss

The changing magnetic field generates current in the iron core, resulting in power loss. The stator and rotor of SRM are constructed in the form of laminated silicon steel sheets, and the insulation is coated between them, which has greatly reduced the eddy current in the core, but the loss caused by eddy current in the silicon steel sheets is still unable to be ignored.

However, for the non-sinusoidal flux density inside the iron core, it is not precise enough to calculate the iron loss simply by peak flux density. In this paper, the time-varying waveform of the flux density on

the stator pole is obtained by combining the FEA, then the magnetic density is integrated in the time period to calculate the eddy current and hysteresis loss. Obviously, this method reflects the influence of non-sinusoidal flux density on iron loss.

As mentioned above, Φ is defined as in the following formula:

$$\Phi = \frac{1}{T}\int_T B(t)dt \tag{3}$$

where T represents the time of one running cycle of SRM.

Since the flux density variation is relatively complex, the following method is adopted to consider the integral of the flux density: Firstly, the 2D FEA of SRM was carried out in ANSYS Maxwell. Then, transient magnetic field analysis was employed to obtain the flux density of the motor at any moment at any point. Finally, the data curve over a period is output to Matlab for integral operation.

Meanwhile, the windings on the stator poles can be considered uniformly arranged, so that the flux density in the stator pole can also be regarded as uniformly distributed except the ends. Therefore, multiplied by the length of the stator pole arc and the length of the stator core, the result is defined as the flux flow as follows:

$$Q = \frac{ac}{T}\int_T B(t)dt \tag{4}$$

where Q is the flux flow on the cross-section of the stator pole, and a and c are the length of stator pole arc (m) and the length of stator core (m), respectively.

In this method, the eddy current and hysteresis losses are generated in the flux path of SRM. And for a three-phase excitation cycle, the windings on the 12 stator poles are excited once, and the total flux path is 12 times L. In addition, the eddy current induced on the silicon steel sheets increases with the aggrandizement of magnetization frequency. Therefore, the following formula is used to calculate the eddy current loss of the whole motor.

$$P_e = 12L \cdot C_e f^2 \frac{ac}{T}\int_T B(t)dt = 12L \cdot C_e f^2 Q \tag{5}$$

where L is the flux path of single stator pole excitation, which is given in (2), C_e the eddy current loss coefficient, f the flux density frequency (Hz), and Q the flux flow in the stator pole, which is given in (4).

2.2. Hysteresis Loss

From a physical point of view, magnetic materials are inclined to retain their magnetism, and ferromagnets do the same. This phenomenon leads to the magnetization in the ferromagnetic body always lagging behind the change of magnetic field strength [15]. Thus, hysteresis loss occurs when magnetic domains in the iron core are repeatedly magnetized.

The magnitude and direction of the flux are always changing due to the periodic motion of SRM, and obviously, this is where the hysteresis loss comes from. Hysteresis loss is also positively correlated with the amplitude of flux density in SRM.

So, the hysteresis loss calculation formula is introduced as

$$P_h = 12LC_h f \cdot \frac{dB(t)}{dt}\Phi \tag{6}$$

where C_h is the hysteresis loss correction coefficient of this calculation model, f the frequency of flux density, and L the flux path of single stator pole excitation.

The variation trend of flux density is not a constant in (6), which brings great difficulty to the accurate calculation of hysteresis loss. Therefore, this paper simplifies the above formula as follows: the flux density curve of the stator pole in a period is decomposed near the extreme points, and each section of the curve is linearly fitted to construct a broken line chart (which may not be closely connected). The piecewise function expression $B(t)$ is written according to the linear fitting curve. Based on this

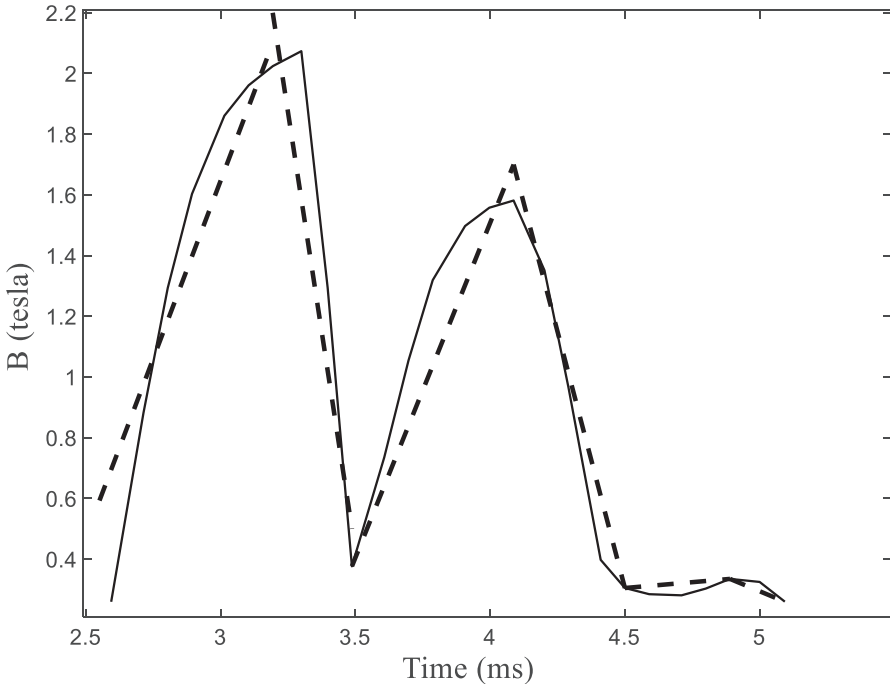

Figure 4. Piecewise linearization of the flux density in stator pole.

method, the hysteresis loss can be obtained from the linear expression of the flux density over a period, as shown in Figure 4.

Since the flux density is fitted as a piecewise linear function, the slope of the broken line in each segment is fixed, i.e., $dB(t)/dt$ is a constant in each segment. Equation (6) can be rewritten as

$$\begin{aligned} P_h &= 12LC_h f \sum_{k}^{M} \left\{ \left| \frac{dB_k(t)}{dt} \right| \cdot \frac{1}{T_k} \int_{T_k} B_k(t)dt \right\} \\ &= 12LC_h f \sum_{k}^{M} \left\{ p_k \cdot \frac{1}{T_k} \int_{T_k} B_k(t)dt \right\} \end{aligned} \tag{7}$$

where k represents each fitting subsection of the flux density curve; M is the total number of subsection, i.e., the number of subsection expressions; p_k is the change rate of flux density at segment k, namely the slope of each segment of the linear fitting curve; T_k and $B_k(t)$ are the duration and flux density of part k, respectively.

From what has been discussed above, the total iron loss of SRM can be obtained as follows:

$$P_{\text{iron}} = P_e + P_h \tag{8}$$

3. VERIFICATION AND DISCUSSION

In order to verify the developed method, the existing loss separation model and FFT method are applied to make a comparison. The loss separation model is shown in (1), which cannot be used to calculate the core loss under non-sinusoidal magnetic density waveform. However, the FFT method can approximate the core loss in the cases by harmonic decomposition: Assuming that the fundamental frequency of the magnetic density is f, the amplitude of the m-th harmonic is B_{mP}, and the frequency is mf after Fourier transform, then the iron loss caused by the m-th harmonic is:

$$P_{\text{iron}-m} = K_e(mf)^2 B_{mP}^2 + mK_h f B_{mP}^{\alpha} \tag{9}$$

The magnetic density in the motor core is usually given in terms of radial and tangential components. Supposing that the radial component is represented by B_r and the tangential component by B_t, the peak magnetic density of the m-th harmonic component can be expressed as:

$$B_{mP} = \sqrt{B_{rm}^2 + B_{tm}^2} \tag{10}$$

where B_{rm} and B_{tm} are the amplitude of the m-th harmonic of the radial and tangential components, respectively. (10) is substituted into (9), and Eq. (11) can be obtained:

$$P_{\text{iron}-m} = K_e(mf)^2 \left(B_{rm}^2 + B_{tm}^2\right) + mK_h f \left(B_{rm}^2 + B_{tm}^2\right)^{\frac{\alpha}{2}} \tag{11}$$

In addition, the number of harmonics may be infinite after Fourier transform for an actual waveform of magnetic density. The higher the number of harmonics is, the smaller the amplitude is, so when the number of harmonics reaches a certain level, the amplitude is close to zero [16]. In the calculation, the sum of the losses of the first eight harmonics can be taken as the loss of the iron core per unit mass (Figure 5).

$$P_{\text{iron}} = \sum_{m=1}^{8} K_e(mf)^2 \left(B_{rm}^2 + B_{tm}^2\right) + \sum_{m=1}^{8} mK_h f \left(B_{rm}^2 + B_{tm}^2\right)^{\frac{\alpha}{2}} \tag{12}$$

Obviously, the separation of harmonic components makes the calculation of iron loss by FFT method more accurate than the original model in SRM. In addition, FEA simulation results will be used as the reference value of iron loss to further compare the differences of the three methods.

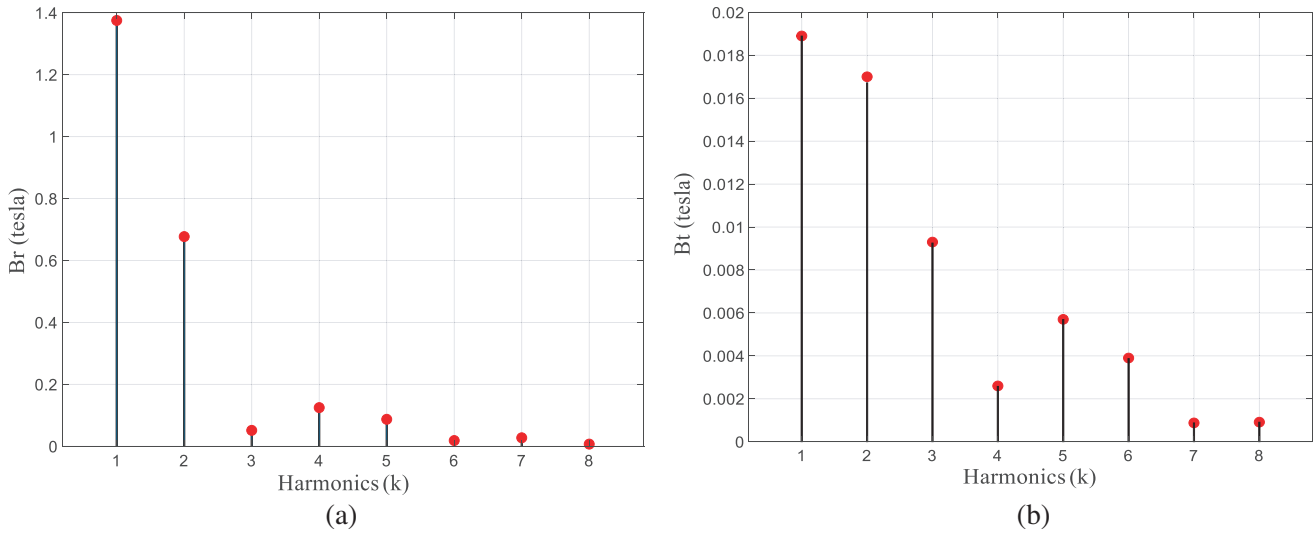

Figure 5. Harmonic components of flux density. (a) Radial components. (b) Tangential components.

In the loss separation model and the improved model combined FFT method, the dual-frequency method [17] can be used to obtain coefficients K_e and K_h without separating eddy current losses and hysteresis losses, as shown below:

$$P_{\text{iron}}/f = K_e a(B) f + K_h b(B) \tag{13}$$

In this paper, a 12/8 SRM is taken as the research object, and the specific parameters of the motor are shown in Table 1. For the SRM, in the range of 100–500 Hz of magnetic frequency, the coefficients can be selected as: $K_e = 0.0001$, $K_h = 0.034$, $\alpha = 1.5$.

To consider the FIP method proposed in this paper, the correction coefficients can also be fitted by measuring iron loss, and C_e and C_h are set to 0.58 and 1.2, respectively.

In the range of 100–500 Hz, the frequencies of 100 Hz, 200 Hz, 300 Hz, 400 Hz, and 500 Hz are selected as the operating frequency points of the motor.

Table 1. Dimensions of the 12/8 SRM.

Parameters	Value
Stator outer diameter (mm)	120
Stator inner diameter (mm)	69.8
Number of stator poles	12
Number of rotor poles	8
Number of turns per pole	50
Rotor outer diameter (mm)	69
Rotor inner diameter (mm)	30
Stator pole embrace	0.5
Rotor pole embrace	0.355
Thickness of stator yoke (mm)	9
Thickness of rotor yoke (mm)	6.7
Stator stack length (mm)	65
Steel material	DW360-50

The eddy current and hysteresis losses are calculated by the loss separation model, the improved model combined FFT method, and the FIP method proposed in this paper, respectively. The results are listed in Table 2, wherein, the first two existing methods calculate the iron loss of stator pole, stator yoke, rotor pole, and rotor yoke respectively and sum them up, which is not presented separately here.

In order to more clearly show the difference among the three methods of iron loss calculation, the data of eddy current loss and hysteresis loss is shown in Figure 6 in the form of a bar chart. As can be seen from Table 2 and Figure 6, with the increase of frequency, the errors of the three methods increase, both in eddy current loss and hysteresis loss. Nevertheless, within this frequency range, the results of the proposed method are in good agreement with those of the other two methods. So, the FIP method has good adaptability to calculate the iron loss in the frequency range of 100–500 Hz.

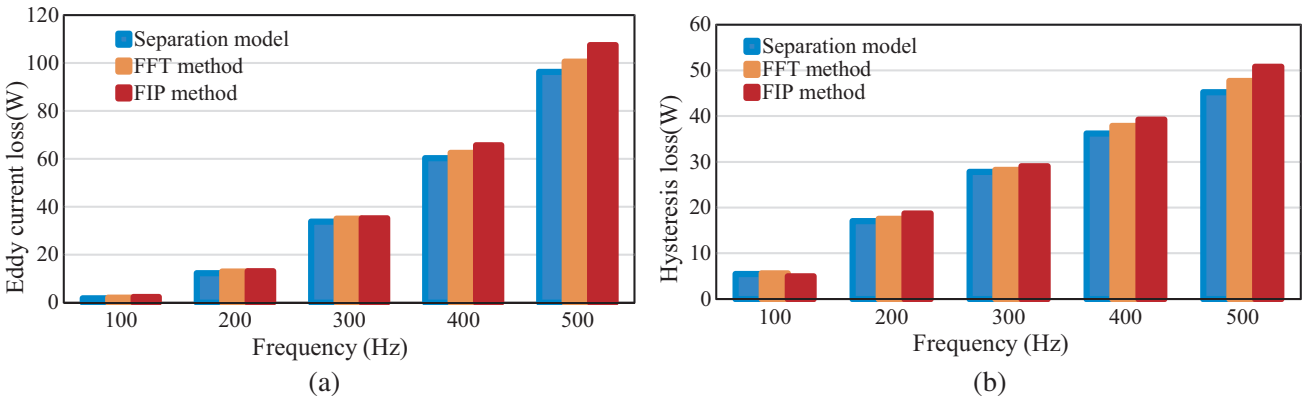

Figure 6. The loss comparison of three analytical methods. (a) Eddy current loss. (b) Hysteresis loss.

In addition, it should be noted that when the magnetization frequency is relatively low, i.e., low speed, hysteresis loss is greater than eddy current loss. However, the eddy current loss exceeds hysteresis loss and becomes the main part of iron loss with the increase of frequency.

Next, the 2D FEA simulation of the SRM at each frequency is carried out in ANSYS Maxwell, and the iron loss is obtained. Then it is compared with the iron loss data calculated by separation model, improved model with FFT method, and the FIP method, as shown in Table 3. The iron loss in the table is the sum of eddy current and hysteresis loss.

Table 2. Eddy current and hysteresis loss results at different frequencies.

Frequency (Hz)	Eddy current loss (W)			Hysteresis loss (W)		
	Separation Model	FFT method	FIP method	Separation Model	FFT method	FIP method
100	1.82	2.14	2.35	5.51	5.63	4.96
200	12.36	1297	13.05	17.06	1755	18.73
300	33.82	3503	35.22	27.82	2824	29.01
400	60.28	6253	65.67	36.17	3786	39.24
500	96.34	10162	107.45	4525	4772	50.8

Table 3. Iron loss of the four methods and errors at different frequencies.

Frequency (Hz)	Iron loss (W)						
	FEA	Separation	Separation-FEA	FFT method	FFT-FEA	FIP method	FIP-FEA
100	8.25	7.33	11.15%	7.77	5.82%	7.31	11.39%
200	31.02	29.42	5.16%	30.52	1.61%	31.88	2.77%
300	66.81	61.64	7.74%	63.27	5.30%	64.23	3.86%
400	108.03	96.45	10.72%	100.39	7.07%	104.91	2.89%
500	157.47	141.59	10.08%	148.34	5.80%	159.25	1.13%

The iron loss results of the four methods are also shown in Figure 7 in the form of a bar chart. Compared with the loss separation model and the improved model, the iron loss calculated by FIP method is closer to the data obtained by FEA simulation. In addition, it can also be seen that when the frequency is high enough (500 Hz), the simulated iron loss is less than that calculated by FIP method, because there will be local saturation of flux density in the motor, and there is no iron loss in this region.

In order to compare the iron loss of different methods more directly, the errors of the loss separation model, improved separation model, and proposed FIP method compared with FEA simulation are shown in Table 3 and the broken lines in Figure 7. The error of the separation-FEA is the maximum at each frequency, while the error of the FIP-FEA decreases significantly at high frequency and is at a low level.

Another important indicator to measure the core loss analysis methods is efficiency. Table 4 shows the iron loss analysis time under different methods. It can be seen that the iron loss calculation of the separation model is the simplest and requires the least time. The model combined with FFT method needs to decompose harmonics, and the calculation time is the longest. Although the method proposed in this paper is not the least in terms of analysis time, it undoubtedly shortens the required time compared with FEA simulation and FFT methods.

Table 4. Iron loss analysis time of different methods at a certain frequency.

	FEA	Separation	FFT method	FIP method
Time (s)	375	103	542	261

The above analyses reflect the high accuracy of FIP method in calculating core loss. Compared with the other two analytical calculation methods, the proposed method considers the magnetic flux density in SRM from the perspective of the whole, which not only avoids the block calculation of iron loss, greatly reduces the calculation amount, but also improves the reliability of calculation.

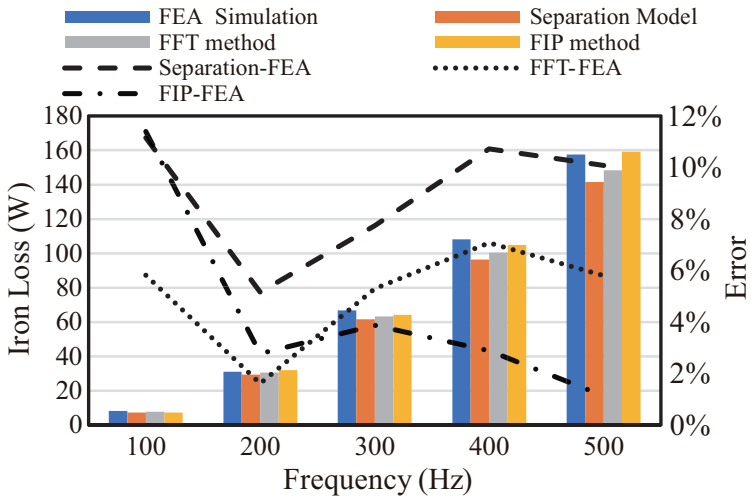

Figure 7. Comparison of core loss and errors between different methods.

4. CONCLUSION

In this paper, a new method of calculating iron loss, the FIP method, is proposed, and the formulas for eddy current and hysteresis losses are given, respectively. First of all, the flux path in the closed loop of the motor is abstracted, and the periodic flux density of the stator pole is integrated in time to calculate the iron loss of the whole motor. Then, the concept of flux flow on the stator pole cross-section is introduced into the calculation method of eddy current loss. In order to investigate the flux density variation during the hysteresis loss calculation, the piecewise linear fitting of the flux density is carried out. In the proposed method, the flux density on the stator pole is obtained by finite element simulation, which will bring convenience to the calculation of iron loss and make the results more accurate. The correctness and practicability of the proposed method are proved by comparing the FIP method with the existing loss separation model, improved separation model, and FEA simulation. It can be concluded that the FIP method is more accurate and more stable than others, and it does not need to block SRM and does not need to consider the complex flux density distribution of each part of the motor, but only needs to calculate once, which greatly simplifies the calculation steps, and is simpler and more effective.

REFERENCES

1. Hu, J., Y. Wang, H. Fujimoto, and Y. Hori, "Robust yaw stability control for in-wheel motor electric vehicles," *IEEE-ASME Trans. Mechatron.*, Vol. 22, No. 3, 1360–1370, June 2017.
2. Valdivia, V., R. Todd, F. J. Bryan, A. Barrado, A. Lázaro, and A. J. Forsyth, "Behavioral modeling of a switched reluctance generator for aircraft power systems," *IEEE Trans. Ind. Electron.*, Vol. 61, No. 6, 2690–2699, June 2014.
3. Li, Z., X. Yu, Z. Qian, X. Wang, Y. Xiao, and H. Sun, "Generation characteristics analysis of deflection type double stator switched reluctance generator," *IEEE Access*, Vol. 8, 196175–196186, 2020.
4. Yamazaki, K. and K. Kanbayashi, "Shape optimization of induction machines by using combination of frequency- and time-domain finite element methods," *IEEE Transactions on Magnetics*, Vol. 49, No. 5, 2185–2188, May 2013.
5. Mthombeni, L. T., P. Pillay, and N. A. Singampalli, "Lamination core loss measurements in machines operating with PWM or nonsinusoidal excitation," *IEEE International Electric Machines and Drives Conference 2003, IEMDC'03*, Vol. 2, 742–746, 2003.

6. Lavers, J., P. Biringer, and H. Hollitscher, "A simple method of estimating the minor loop hysteresis loss in thin laminations," *IEEE Transactions on Magnetics*, Vol. 14, No. 5, 386–388, September 1978.
7. Hayashi, Y. and T. J. E. Miller, "A new approach to calculating core losses in the SRM," *IEEE Trans. Ind. Appl.*, Vol. 31, No. 5, 1039–1046, September–October 1995.
8. Ganji, B., Z. Mansourkiaee, and J. Faiz, "A fast general core loss model for switched reluctance machine," *Energy*, Vol. 89, 100–105, 2015.
9. Faiz, J., B. Ganji, C. E. Carstensen, and R. W. De Doncker, "Loss prediction in switched reluctance motors using finite element method," *Eur. Trans. Electr. Power*, Vol. 19, No. 5, 731–748, July 2009.
10. Bouchnaifa, J., K. GrariaAnas, A. Benslimaneb, and F. Jeffali, "Analytical approach and thermal signature of Switched reluctance motor iron losses," *Materials Today: Proceedings*, Vol. 27, No. 4, 3161–3166, 2020.
11. Shen, W., F. Wang, D. Boroyevich, and C. W. Tipton, "Loss characterization and calculation of nanocrystalline cores for high-frequency magnetics applications," *IEEE Trans. Power Electron.*, Vol. 23, No. 1, 475–484, January 2008.
12. Yu, Q., B. Bilgin, and A. Emadi, "Loss and efficiency analysis of switched reluctance machines using a new calculation method," *IEEE Trans. Ind. Electron.*, Vol. 62, No. 5, 3072–3080, May 2015.
13. Yan, W., H. Chen, Y. Liu, and C. Chan, "Iron loss and temperature analysis of switched reluctance motor for electric vehicles," *IET Electr. Power Appl.*, Vol. 14, No. 11, 2119–2127, 2020.
14. Shahriari Nasab, P., M. Moallem, E. Shirani Chaharsoghi, C. Caicedo-Narvaez, and B. Fahimi, "Predicting temperature profile on the surface of a switched reluctance motor using a fast and accurate magneto-thermal model," *IEEE Trans. Energy Convers.*, Vol. 35, No. 3, 1394–1401, September 2020.
15. Sixdenier, F., L. Morel, and J. P. Masson, "Introducing dynamic behavior of magnetic materials into a model of a switched reluctance motor drive," *IEEE Transactions on Magnetics*, Vol. 42, No. 3, 398–404, March 2006.
16. Petrea, L., C. Demian, J. F. Brudny, and T. Belgrand, "High-frequency harmonic effects on low-frequency iron losses," *IEEE Transactions on Magnetics*, Vol. 50, No. 11, 1–4, November 2014.
17. Yang, L., C. Liu, and J. Yan, "A study on iron loss finite element analysis of switched reluctance motor based on a double-frequency method," *Proceedings of the CSEE*, Vol. 26, No. 12, 117–121, June 2006.